Measurement of the collision time of dense electronic plasma induced by a femtosecond laser in fused silica

Article *in* Optics Letters · February 2005

DOI: 10.1364/OL.30.000320

6 authors, including:

Quan Sun
Hokkaido University

Hongbing Jiang
Peking University

Zhaoxin Wu
Xi'an Jiaotong University

Measurement of the collision time of dense electronic plasma induced by a femtosecond laser in fused silica

Quan Sun, Hongbing Jiang, Yi Liu, Zhaoxin Wu, Hong Yang, and Qihuang Gong

State Key Laboratory for Mesoscopic Physics and Department of Physics, Peking University, Beijing 100871, China

Received June 16, 2004

Electronic plasma induced by a focused femtosecond pulse (130 fs, 800 nm) in fused silica was investigated by use of pump–probe technology. Pump and probe shadow imaging and interferometric fringe imaging were combined to determine electronic collision time τ in the conduction band, and τ was measured to be 1.7 fs at an electron density near 5×10^{19} cm^{-3}. The lifetime of the electronic plasma is also measured to be ~170 fs by use of the time-resolved shadow imaging technique.

OCIS codes: 320.0320, 190.7110, 350.5400, 320.7130.

The interaction and propagation of focused femtosecond laser pulses in transparent dielectric materials attracted great attention recently. Many interesting phenomena, such as filamentation,[1–3] pulse splitting,[4] supercontinuum generation,[5] soliton generation,[6] and pulse compression,[7,8] were found to be associated with electron plasma induced by a femtosecond laser, which depended strongly on a nonlinear ionization process. For subpicosecond laser pulses, there are two mechanisms[9,10] for nonlinear ionization: photoionization and avalanche ionization. For avalanche ionization the conduction electrons should obtain enough energy by absorbing photons through electron collision (inverse bremsstrahlung) to excite more electrons into the conduction band. Thus electronic collision time τ in the conduction band is an important parameter for exploration of the underlying mechanisms of femtosecond interaction with transparent materials. Collision time τ is determined by the electron–phonon scattering rate. Arnold *et al.* pointed out theoretically that electron momentum relaxation rates in SiO_2 thin film are energy dependent, varying by 2 orders of magnitude.[11] The corresponding value of τ is approximately 10^{-16}–10^{-14} s. However, this value of τ has not been measured experimentally. Various magnitudes of τ were employed in different reports and calculations; for example, Sudrie *et al.*[1] used 23.3 fs and Tzortzakis *et al.*[2] used 10 fs (obtained from the inverse bremsstrahlung cross section $\sigma = 2.78 \times 10^{-18}$ cm^2). Meanwhile, another parameter, mean electron-number density, was measured by shadow imaging. Interestingly, the formula used to determine the electron density (n_e) from a shadowgraph is also related to τ, which was assigned a value of 0.2 fs by Mao *et al.*[12]

As is well known, interferometric fringe measurement is another effective method for plasma diagnostics.[13,14] Interferometric measurement will provide n_e independent of τ. Thus, in this Letter, we combined shadow measurement with interferometric fringe measurement to diagnose plasma and, surprisingly, obtained an electronic collision time τ in fused silica of 1.7 fs at an electron density near 5×10^{19} cm^{-3}. In addition, electron plasma lifetime τ_e was also measured to be 170 fs in fused silica; this is in good agreement with the measurement performed by Audebert *et al.*[15] They used a sensitive technique based on interference in the frequency domain to measure the τ_e as ~150 fs, a value that has been cited widely.

In our experiment a Ti:sapphire chirped-pulse amplification laser with a pulse duration of 130 fs, wavelength of 800 nm, and repetition rate of 10 Hz was used. A schematic diagram of the experimental setup of a time-resolved shadowgraph and an interferometric measurement is shown in Fig. 1. A shutter controlled by a computer was used to obtain a single pulse. The laser beam was then split into pump and probe pulses by a beam splitter. Objective A (Olympus, 4×, 12-mm working distance) with a numerical aperture (NA) of 0.16 was used to focus the pump laser beam. The sample was a piece of 3 mm × 5 mm × 20 mm fused silica with polished surfaces, and it could be translated perpendicularly to the propagation direction of the pump and the probe beams to avoid multi-interaction. The interaction region was inside the sample, approximately several hundred millimeters from the front surface. The probe beam passed an optical delay stage and a polarizer and illuminated the interaction region perpendicularly to the pump beam. The transmitted probe beam was imaged onto a CCD by another objective, B (20×, NA of 0.4). For interferometric measurement, a Wollaston prism with its optical axis 45° to the polarization direction of the incident probe

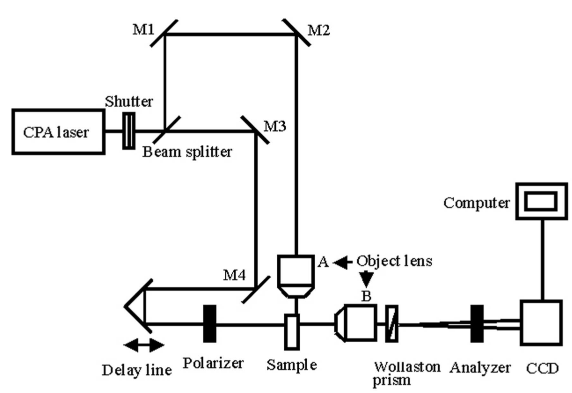

Fig. 1. Experimental setup of the shadowgraph (without a Wollaston prism and an analyzer) and the interferometric measurement. CPA, chirped-pulse amplification; M1–M3, mirrors.

beam was utilized after object B to split the probe beam into two beams with 2° separation. Then the two beams passed an analyzer with its polarization direction parallel to the polarizer to form the interference fringes. In the experiments time zero was set when the peaks of the pump beam and the probe beam overlapped at $z = 0$.

Figure 2 shows four shadowgraphs measured at different delay times, the laser intensity being $\sim 7 \times 10^{13}$ W/cm^2 in the focal region. The pump beam propagated from right to left. The filaments were observed, and the evolution of electron plasma was obtained. Considering that the plasma density has cylindrical symmetry along the pump beam, the probe beam would undergo absorption, reflection, and refraction when it passes through the plasma region. The incidence angle of the central part of the probe laser, which passes through the axes of the plasma, is equal to zero, so the refractive effect can be neglected. Moreover, the reflective effect is also insignificant, which will be explained below. Thus we can consider only the absorption effect, and the central part of the probe laser's intensity I_p follows

$$\mathrm{d}I_p/\mathrm{d}x = -\alpha I_p = -\sigma n_e I_p\,, \tag{1}$$

where σ is the absorption cross section for inverse bremsstrahlung, according to the Drude model[9]:

$$\sigma = \frac{ke^2\tau}{m_e\epsilon_0\omega[1 + (\omega\tau)^2]}\,. \tag{2}$$

In Eq. (1), x is along the direction of the probe beam. In Eq. (2), $k = 2\pi n_0/\lambda$, where n_0 is the refractive index of the fused silica; λ is the vacuum wavelength of the probe laser; and m_e, ϵ_0, and ω represent the electron mass, the vacuum dielectric constant, and the frequency of the laser, respectively. However, τ in fused silica has not been measured in previous experiments to our knowledge. We obtain its value associated with the interferometric measurement, as discussed below.

The integral of Eq. (1) is

$$\frac{1}{\sigma}\ln\frac{I_{p0}}{I_{pd}} = \int n_e \mathrm{d}x\,. \tag{3}$$

Here I_{p0} and I_{pd} represent the probe laser intensity without and with passing through the plasma region.

In the interferometric method, the probe beam is split into two beams by the Wollaston prism and forms an interferometric fringe on the image plane after it passes through an analyzer. When the probe beam traverses the plasma region, the induced phase shift of the probe beam can be expressed as[13]

$$\Delta\varphi = \int (n - n_0)\omega/c\mathrm{d}x = \frac{\omega}{2cn_c}\int n_e\mathrm{d}x = 2\pi D\,, \tag{4}$$

where n and n_0 indicate the refractive indices with and without plasma in fused silica, respectively; $n_c = \epsilon_0 m_e\omega^2/e^2 = 1.7 \times 10^{21}$ cm^{-3} is the critical electron density of an 800-nm probe laser; and D is the fringe shift number. We evaluated a plasma density of the order of 5×10^{19} cm^{-3} by use of Eq. (4). Now we can discuss the loss of the probe beam as a result of reflection. We assume the average plasma density to be 5×10^{19} cm^{-3}. Then the difference of refractive index caused by plasma $\Delta n = n_e/2n_c \approx 0.03$. When the incidence angle is zero, the reflectivity of probe beam $R \approx (\Delta n/2n_0)^2 \approx 0.01\%$. So when we acquire I_{p0}/I_{pd} in the axis of the plasma in the shadowgraph, the loss of I_p is mostly caused by absorption of the plasma.

Equations (2) and (4) have the same integrating format. So we can easily obtain Eq. (5), from which τ is determined by measurement of the probe-beam intensity transmittance I_{pd}/I_{p0} from the shadowgraphs and fringe shift number D from the interferometric image:

$$\frac{\ln(I_{p0}/I_{pd})}{4\pi n_0 D}\,\frac{1 + (\omega\tau)^2}{\omega\tau} - 1 = 0\,. \tag{5}$$

Figure 3 shows an interferometric image at a delay time of 400 fs. The fringe interval is calculated to be 12.5 pixels, and the fringe shift is 2 ± 0.5 pixels at $z = 92$ μm. So D is 0.16 ± 0.04. The corresponding probe-beam intensity transmittance I_{pd}/I_{p0} from the corresponding shadowgraph in Fig. 2 is 0.445 at the same point and at the same delay time. Then, the result of τ is calculated to be 1.4 ± 0.4 fs. Here the

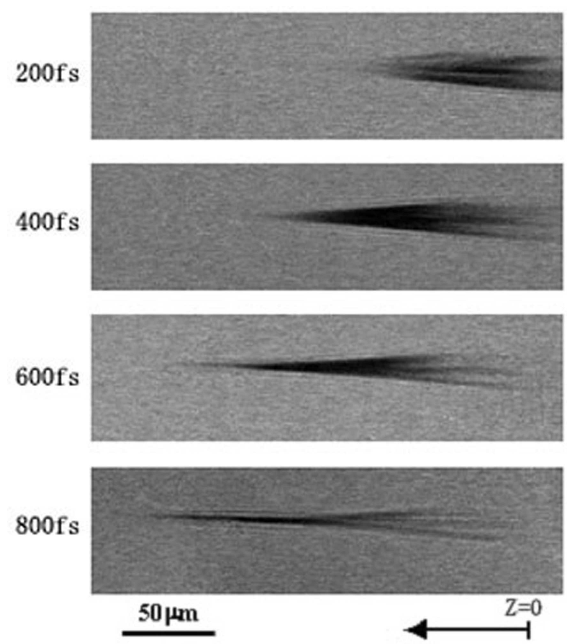

Fig. 2. Time-resolved shadowgraphs for femtosecond laser-induced plasma in fused silica. The intensity is $\sim 7 \times 10^{13}$ W/cm^2 in the focal region.

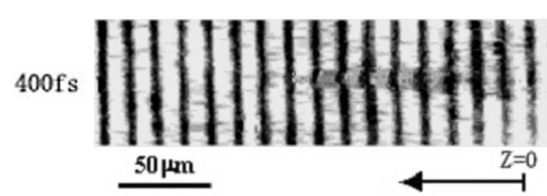

Fig. 3. Interferometric image for femtosecond laser-induced plasma in fused silica at a 400-fs delay time; the intensity is also $\sim 7 \times 10^{13}$ W/cm^2 in the focal region.

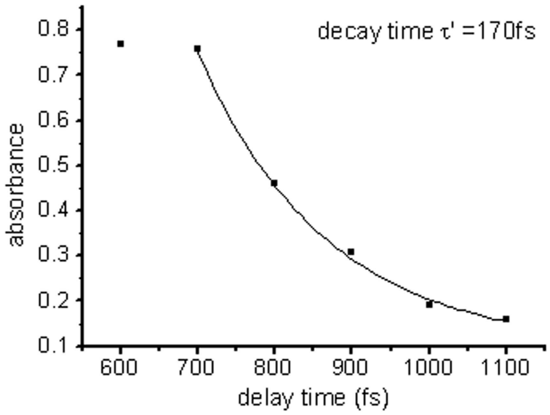

Fig. 4. Evolution of absorption of the probe beam due to electron plasma at the $z = 119\ \mu$m position. The vertical axis represents absorbance, denoted by $\ln(I_{p0}/I_{pd})$. The solid curve indicates the exponential decay fitting with a decay time of 170 fs.

primary measurement error comes from the choice of the value of the fringe shift. The fringe shift error may be considered to be ± 0.5 pixels in our experiments. At different time delays, we measured three other values of τ to be 1.3 ± 0.4 fs, 1.7 ± 0.5 fs, 2.5 ± 0.7 fs. The average collision time τ is 1.7 fs. This difference of measured τ values may be due to two factors. One is the measurement error mentioned above. Another factor may be the different electron distributions in the conduction band at different delay times. After the probe pulse passes the interaction region, the energy of conduction electrons decreases with time because of electron–phonon collision. The larger τ value corresponds to a longer delay time, i.e., to lower kinetic energy of conduction electrons. This variation is compatible with the calculations of Arnold *et al.*[11] According to their results, the relaxation rate increased monotonically with an increase in the electron's kinetic energy when the kinetic energy was below 6 eV, and the average kinetic energy in our experiment was estimated to be within this energy range.

In addition, according to Eqs. (1) and (3) the parameter $\ln(I_{p0}/I_{pd}) = \int \alpha \mathrm{d}x$ denotes absorbance. In Fig. 4 we present the time-dependent absorbance of the probe pulse at $z = 119\ \mu$m. When the data points are fitted with exponential decay, a decay time τ_e of 170 fs is obtained. The first several degressive data points were ignored because at that time the electron plasma was still being induced, although the total density was decreasing. We also ignored data points for the delay time that were >1.2 ps, when the thermal effect began to work.

In summary, we have investigated electronic plasma induced by a focused single femtosecond laser pulse in fused silica. We first measured the electron collision time τ in fused silica by use of the interference pattern associated with the shadowgraph of the generated plasma. The measured mean value was 1.7 fs when n_e is of the order of 10^{19} cm^{-3}. Evolution of the electron plasma was observed, and the lifetime of the electron plasma τ_e was determined to be $\sim$170 fs. These data and this analysis are helpful for understanding the fundamental physical mechanisms of femtosecond laser interaction with transparent materials.

This work was supported by National Key Basic Research Special Foundation grant TG1999075207 and by National Natural Science Foundation of China grants 10104003, 90101027, and 10328407.
H. Jiang's e-mail address is hbjiang@pku.edu.cn; Q. Gong's e-mail address is qhgong@pku.edu.cn.

References

1. L. Sudrie, A. Couairon, M. Franco, B. Lamouroux, B. Prade, S. Tzortzakis, and A. Mysyrowicz, Phys. Rev. Lett. **89,** 186601 (2002).
2. S. Tzortzakis, L. Sudrie, M. Franco, B. Prade, and A. Mysyrowicz, Phys. Rev. Lett. **87,** 213902 (2001).
3. Z. X. Wu, H. B. Jiang, L. Luo, H. C. Guo, H. Yang, and Q. H. Gong, Opt. Lett. **27,** 448 (2002).
4. J. K. Ranka, R. W. Schirmer, and A. L. Gaeta, Phys. Rev. Lett. **77,** 3783 (1996).
5. A. Brodeur and S. L. Chin, Phys. Rev. Lett. **80,** 4406 (1998).
6. I. G. Koprinkov, A. Suda, P. Wang, and K. Midorikawa, Phys. Rev. Lett. **84,** 3847 (2000).
7. H. Ward and L. Berge, Phys. Rev. Lett. **90,** 053901 (2003).
8. Z. X. Wu, H. B. Jiang, Q. Sun, H. Yang, and Q. H. Gong, Phys. Rev. A **68,** 063820 (2003).
9. B. C. Stuart, M. D. Feit, S. Herman, A. M. Rubenchik, B. W. Shore, and M. D. Perry, Phys. Rev. B **53,** 1749 (1996).
10. B. Rethfeld, Phys. Rev. Lett. **92,** 187401 (2004).
11. D. Arnold, E. Cartier, and D. J. DiMaria, Phys. Rev. B **45,** 1477 (1992).
12. X. Mao, S. S. Mao, and R. E. Russo, Appl. Phys. Lett. **82,** 697 (2003).
13. H. Yang, J. Zhang, Y. J. Li, J. Zhang, Y. T. Li, Z. L. Chen, H. Teng, Z. Y. Wei, and Z. M. Sheng, Phys. Rev. E **66,** 016406 (2002).
14. S. V. Garnov, A. A. Malyutin, O. G. Tsarkova, V. I. Konov, S. M. Klimentov, and F. Dausinger, Proc. SPIE **4637,** 31 (2002).
15. P. Audebert, P. Daguzan, A. D. Santos, J. C. Gauthier, J. P. Geindre, S. Guizard, G. Hamoniaux, K. Krastev, P. Martin, G. Petite, and A. Antonetti, Phys. Rev. Lett. **73,** 1990 (1994).